Dynamical Study of Mechanistic Details in Organic Reactions. II. An Overall Study of Isomerizations of Cyclopropane

Xavier Chapuisat and Yves Jean*

Contribution from the Laboratoire de Chimie Théorique,[1] Université de Paris-Sud, Centre d'Orsay, 91405 Orsay, France. *Received March 1, 1975*

Abstract: A dynamical study of optical and geometrical isomerizations of cyclopropane, including all the main degrees of freedom (ring opening and rotations of the terminal groups), is performed. First, the ab initio potential energy surface for these reactions and the fitting analytical formula used in the dynamical equations are presented. A wide range of initial conditions is studied. Three conclusions emerge: (i) All the dynamical trajectories are closely connected to the general reaction path generated by the static quantum mechanical calculations. (ii) The initial methylene "rotational" (actually vibrational) energy required for a trajectory to be reactive is much greater than generally expected. Furthermore, two distinct "reactive bands" appear, corresponding to values of the initial "rotational" energy of about 18 and 36 kcal/mol, respectively. An interpretation is given for this alternation between "reactive" and "nonreactive" ranges of initial conditions. (iii) For most reactive trajectories, a single rotation of 180° of one or both terminal CH_2 groups occurs within the diradical species before ring closure. The connection of the present study with experiment is briefly discussed.

In a previous article,[2] preliminary dynamical results on geometrical and optical isomerizations of cyclopropane-type molecules were reported. The conditions of this study were somewhat restrictive; the isomerization reactions were not considered as overall reactions, but rather as a sequence of three elementary steps: (i) motion of ring opening of the cyclopropane while all vibrations of both terminal methylene groups are artificially frozen; as a result of this step, the face-to-face (FF) trimethylene is formed; (ii) rotations of the terminal groups within the diradical; this step leads to an isomeric diradical after passage over one or several transition states; (iii) ring reclosure of the isomeric diradical into the reaction product (isomeric cyclopropane molecule). This reaction mechanism is illustrated in Figure 1.

In other terms, the coupling between the motion of the methylene groups (either vibrations or rotations) and the ring-opening or ring-closure motion was neglected. Thus, two partial potential energy surfaces were used separately. From the first one derived the forces which drove the motion of ring opening from cyclopropane to the diradical FF (or the reverse), i.e., steps (i) and (iii). This partial surface included the other molecular geometry parameter which appeared to vary significantly during these steps, i.e., the symmetric change of pyramidalization of the methylene groups between the cyclopropane and the diradical FF (see Figure 9 in ref 2). The second partial potential energy surface was used to study the coupled rotations of the terminal groups within the diradical at constant ring angle ∠CCC, i.e., step (ii). There was no coupling to allow passage from one surface to the other.

From a static point of view, this reaction scheme is justified since quantum-mechanical calculations have shown that the terminal groups are energetically forbidden from rotating as long as the carbon ring is not sufficiently opened.

The present article aims at studying the overall reaction of isomerization of cyclopropane by means of a complete potential energy surface, including simultaneously all the important geometrical degrees of freedom of the molecule. We must first adequately select these degrees of freedom.

The Static Surface

Dimensions of the Problem and Nature of the Potential Energy Surface. Ideally, we would like to retain and treat simultaneously all the degrees of freedom which intervened in the two separate parts of the previous study. Two such dimensions were associated with the ring opening: the carbon ring angle ($\angle CCC = 2\alpha$) and an angle (β_0) specifying the state of pyramidalization of the terminal methylene groups. In fact two different angles β_1 and β_2 should have been taken into account but they were reduced to one angle β_0 such that $\beta_1 = \beta_2 = \beta_0$, which means that the pyramidalization was artificially held symmetric throughout the motion. For the rotation of FF, two other degrees of freedom appeared: θ_1 and θ_2, the angles of rotation of the terminal methylene groups around the adjacent carbon–carbon bonds.

However, bringing together these two surfaces is not a straightforward matter. A five- (and not four-) dimensional potential energy surface must indeed be considered. The angles β_1 and β_2 will not remain equal as soon as rotations occur in the meantime. Thus, if five were not too large a number for the dimensions of a problem in organic chemical dynamics, we should look for a five-dimensional potential energy surface:

$$V(\alpha,\beta_1,\theta_1,\beta_2,\theta_2) \qquad (1)$$

Moreover our previous dynamical experience (and our chemical intuition) shows that β_1 and β_2 are dynamically much less important coordinates than θ_1 and θ_2. We will therefore consider β_1 and β_2 not as independent dynamical variables, but as adiabatic functions $\beta_1(\alpha,\theta_1)$ and $\beta_2(\alpha,\theta_2)$, respectively. Such an artifact was already used in the previous article[2] for the rotational motion, where β_1 and β_2 were considered as adiabatic functions of θ_1 and θ_2, respectively.

Thus the simplification consists in finding a unique adiabatic function $\beta'(\alpha,\theta)$. From the previous potential energy surface for ring opening in α,β_0 at $\theta_1 = \theta_2 = 0$ (cf. Figure 10 in ref 2), we keep only the minimum energy path: $\beta_0 = \beta_0(\alpha)$ (all the dynamical trajectories deviated little from it). An important requirement must be fulfilled (cf. Figure 2): at constant value of α, the pyramidalization function $\beta'(\alpha,\theta)$ must invert algebraically between $\theta = 0$ and 180° (through a nonpyramidalized state at $\theta = 90°$), in order to have the correct physical behavior. The pyramidalization angle, which is the only physically meaningful quantity, is $|\beta'|$ (cf. Figure 2), so that:

$$\beta_i(\alpha,\theta_i) = |\beta'(\alpha,\theta_i)| \qquad (i = 1, 2) \qquad (2)$$

Practically, the values of β' used in order to compute the

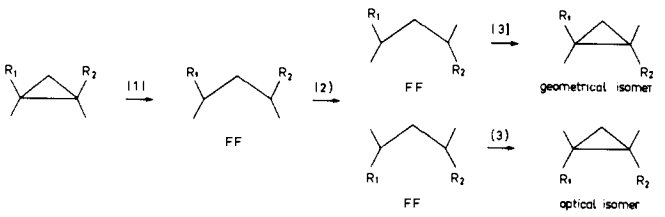

Figure 1.

potential energy function V are linearly interpolated between the only values which are reliable, i.e., $\beta_0(\alpha)$ at $\theta = 0$, 0 at $\theta = \pi/2$ and $-\beta_0(\alpha)$ at $\theta = \pi$:

$$\beta'(\alpha,\theta) = \beta_0(\alpha)(1 - [2\theta/\pi]) \quad (3)$$

Consequently, the three-dimensional potential energy function which will be used throughout the present study is:

$$V(\alpha,\theta_1,\theta_2) = V(\alpha,\beta_1(\alpha,\theta_1),\theta_1,\beta_2(\alpha,\theta_2),\theta_2) \quad (4)$$

Analytical Expression of the Three-Dimensional Potential Energy Function. The potential energy function $V(\alpha,\theta_1,\theta_2)$ can be rewritten as a sum of two terms:

$$V(\alpha,\theta_1,\theta_2) = V(\alpha,0,0) + [V(\alpha,\theta_1,\theta_2) - V(\alpha,0,0)] \quad (5)$$

The first term corresponds to the potential energy of a cyclopropane molecule in the FF configuration, with the ring angle $\angle CCC = 2\alpha$ (Figure 3a). The second term denotes the amount of energy required for rotations of the terminal CH_2, with angular amplitudes of θ_1 and θ_2, at constant α. For this last term, we use the same type of analytical expression which described the rotation potential energy surface at $2\alpha = 113°$ in the previous study.[2] However, the constant parameters a, b, c, and d which appeared in this formula now become functions of α:

$$V(\alpha,\theta_1,\theta_2) = V_0(\alpha) + a(\alpha)\sin^2(\theta_1 + \theta_2)\sin^2(\theta_1 - \theta_2) + b(\alpha)\sin^2(\theta_1 - \theta_2)\cos^2(\theta_1 + \theta_2) + c(\alpha)\sin^2(\theta_1 + \theta_2)\cos^2(\theta_1 - \theta_2) + d(\alpha)\sin^2\theta_1\sin^2\theta_2 \quad (6)$$

where

$$V_0(\alpha) = V(\alpha,0,0) \quad (7)$$

The function $a(\alpha)$ denotes the potential energy of the molecule in the configuration EF(α) (Figure 3b) minus the potential energy of FF(α) (Figure 3a). Similarly, $d(\alpha)$ is the potential energy of the molecule in the configuration EE(α) (Figure 3c). $b(\alpha)$ and $c(\alpha)$ are simple functions of the potential energy barriers to the synchronous disrotatory motion [$h_D(\alpha)$] and the synchronous conrotatory motion [$h_C(\alpha)$] respectively (see Figure 4):

$$b(\alpha) = [h_D(\alpha) + (h_D^2(\alpha) - h_D(\alpha)d(\alpha))^{1/2}]/2 \quad (8)$$

$$c(\alpha) = [h_C(\alpha) + (h_C^2(\alpha) - h_C(\alpha)d(\alpha))^{1/2}]/2 \quad (9)$$

The functions $V_0(\alpha)$, $a(\alpha)$, $b(\alpha)$, $c(\alpha)$, and $d(\alpha)$ are analytically approximated by means of one-dimensional cubic spline functions.

Quantum-Mechanical Calculation of the Potential Energy Surface. The need for a unique three-dimensional potential required the quantum-mechanical calculation of many new points on the potential energy surface. Essentially it was necessary to calculate several new rotational energy surfaces, for values of α different from the single value 113° used previously.[2] Calculations were performed with a 3 × 3 CI version of GAUSSIAN 70, at the STO-3G level, which has now been described many times elsewhere.[3]

In a first step, the new program was used to recalculate the potential energy obtained by means of the previous (STEVENS) program.[4] At $2\alpha = 113°$, both calculations are in very good agreement for the properties of the rotation potential energy surface. EE(α) is energetically 3.2 kcal/mol (3.7 kcal/mol)[5] above FF(α) taken as origin of the energies, and EF(α) is 5.2 kcal/mol (5.1 kcal/mol); the new rotational barriers are: h_C = 3.4 kcal/mol (3.9 kcal/mol) and h_D = 5.5 kcal/mol (5.5 kcal/mol). Consequently, the barriers for conrotatory and disrotatory closures of EE(α) are respectively 0.2 and 2.3 kcal/mol. They are located at 58° (65°) and 50° (53.5°) from FF(α), respectively. Moreover, the diradical FF(α) lies 50.9 kcal/mol (48.4 kcal/mol) above cyclopropane if the 3 × 3 CI is performed only on the diradical, and 56.4 kcal/mol (53.0 kcal/mol) if the CI is performed also for cyclopropane. For the ring-opening (or closure) motion, the energy curve $V_0(\alpha)$ has also been recalculated. It exhibits the same properties as the previous one (see Figure 5): first, there appears no barrier to the reclosure motion of the diradical FF(α); second, the potential energy varies very smoothly in the diradical region ($2\alpha > 90°$), except for very great values of α where strong strains are imposed to the hybridization of the central carbon atom and result in a steeper variation of the potential energy.

Table I. SCF Values of EF(α), EE(α), $h_C(\alpha)$, and $h_D(\alpha)$[a]

2α, deg	$a(\alpha)$ (EF(α))	$d(\alpha)$ (EE(α))	$h_C(\alpha)$	$h_D(\alpha)$
136.1	−2.6	−6.4	0.0	0.0
130.3	−1.8	−5.5	0.0	0.2
124.6	−0.5	−3.4	0.0	0.9
118.9	2.0	−0.4	0.7	2.6
113.2	5.2	3.2	3.4	5.5
107.4	9.3	7.9	8.1	9.2
101.7	15.4	14.8	15.1	15.4
96.0	24.2	25.0	25.9	25.6
90.2	37.1	40.6	41.2	40.6
84.5	55.7	64.4	65.1	64.4
78.8	84.4	104.2	104.8	104.2
73.1	125.0	169.4	170.0	169.4

[a] The numerical values are in kcal/mol and correspond to the energy difference between the actual conformation and that of FF(α).

We now turn to the new points. For 16 values of 2α, regularly spaced from 50.1° = 0.875 rad to 136.1° = 2.375 rad, the potential energy curves which drive (i) the synchronous conrotatory motion of both terminal methylene groups, (ii) the synchronous disrotatory motion, and (iii) the rotation of a single methylene group (the other being held fixed) were computed. The boundaries of 2α are chosen in order to include in our computed potential energy surface all the regions which are energetically attainable if the molecule has enough internal energy to go through any of the transition states, with a maximum excess energy of 10 kcal/mol.

The computed values of $a(\alpha)$, $d(\alpha)$, $h_C(\alpha)$, and $h_D(\alpha)$ for $2\alpha > 1.275$ rad are reported in Table I. For smaller values of 2α, there appears a computational convergence difficulty to obtain the potential energies of the configurations EE(α) and EF(α). This difficulty is put in order in details later.

Comparison of the Potential Energies of FF(α) with that of the Halfway Points EE(α) and EF(α). For values of 2α less or equal to 1.975 rad (113°), both $a(\alpha)$ and $d(\alpha)$ are positive; this means that FF(α) is then the most stable conformation of the diradical. When 2α = 2.075 rad (119°), $d(\alpha)$ becomes negative; now EE(α) is the most stable conformation. Lastly, at 2α = 2.175 rad (125°), both EE(α) and EF(α) are more stable than FF(α).

Comparison of the Rotational Barriers $h_C(\alpha)$ and $h_D(\alpha)$. Within the diradical region ($2\alpha > 100°$), the highest occupied molecular orbital of the planar diradical is antisymmetric with respect to the bisecting plane of symmetry which is perpendicular to the plane of the carbon ring.[7] Consequently, going from FF(α) to EE(α) occurs preferentially in a

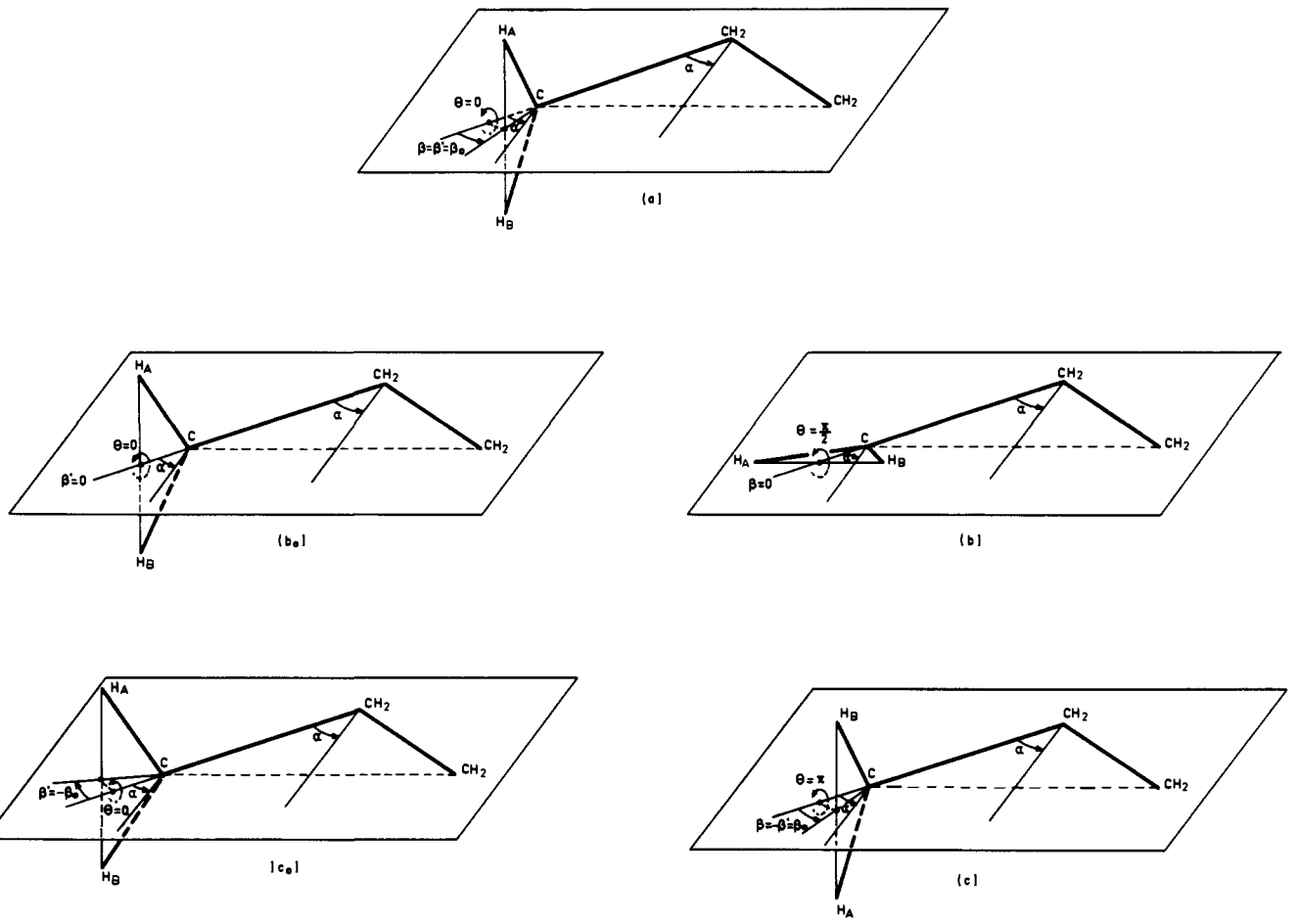

Figure 2. Pyramidalization inversion of a terminal methylene group, when rotating around the adjacent carbon-carbon bond. The true geometries used in computing the potential energy surface at different stages of the motion are illustrated in: (a) $\theta = 0$; (b) $\theta = \pi/2$; and (c) $\theta = \pi$. (b_0) and (c_0) are just given as construction intermediates; they show how the angle β' (cf. eq 2 and 3) determines the state of pyramidalization before rotation.

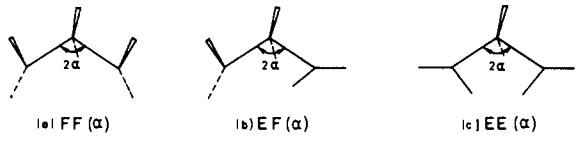

Figure 3. Definition of the geometries of the three diradicals face-to-face (FF(α)), edge-to-face (EF(α)) and edge-to-edge (EE(α)).

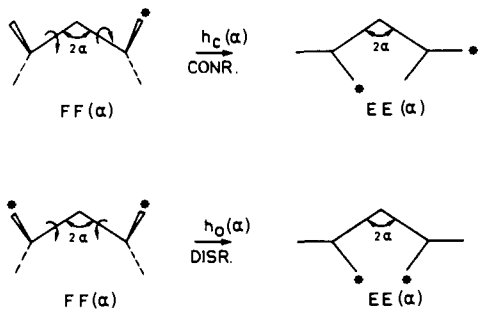

Figure 4.

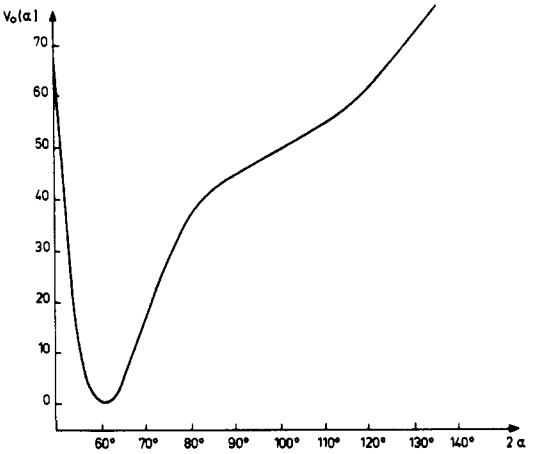

Figure 5. Potential energy curve for the ring opening from cyclopropane to the face-to-face diradical. The energies are in kcal/mol.

conrotatory way. The energy gap between $h_C(\alpha)$ and $h_D(\alpha)$ is maximal when $2\alpha = 1.975$ rad (113°); then it equals 2.1 kcal/mol. For values of 2α smaller than 1.775 rad (102°), the opposite situation is observed. This is due to the crossing, close to $2\alpha \simeq 100°$, of the frontier molecular orbitals in the planar diradical.[7] The symmetric molecular orbital becomes more stable than the antisymmetric one, so that the synchronous disrotatory motion is now preferred to the conrotatory motion. However, the energy gap between $h_C(\alpha)$ and $h_D(\alpha)$ remains small; the preference for the disrotatory motion appears noticeably only at small values of the rotation angles θ_1 and θ_2. In addition, it is worthwhile to note that, for $2\alpha \geq 2.175$ rad, FF(α) is the least stable conformation of the diradical. Then, only the synchronous disrotatory motion requires an activation energy (which is small); the other basic motions occur with a continuous decrease of the potential energy. When $2.175 \text{ rad} > 2\alpha \geq 1.775$ rad, the synchronous conrotatory motion is the one requiring the least amount of activation energy. Last of all,

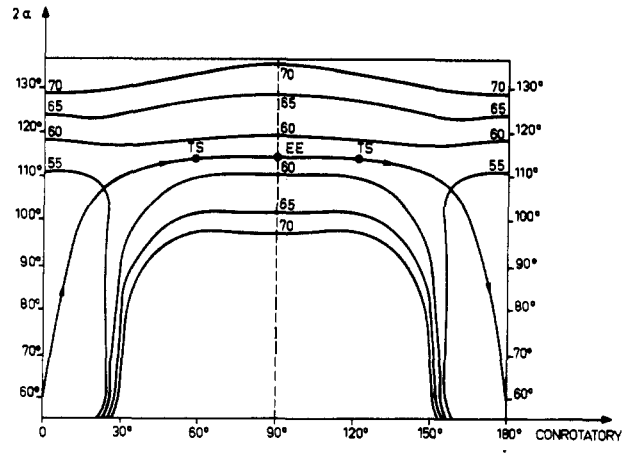

Figure 6. Two-dimensional potential energy surface and static reaction path for the synchronous conrotatory motion of the terminal methylene groups. 2α represents the value of the carbon ring angle. The abcissa gives the common value of both rotational angles: $\theta = \theta_1 = \theta_2$. TS denotes the position of a transition state. The energies are in kcal/mol.

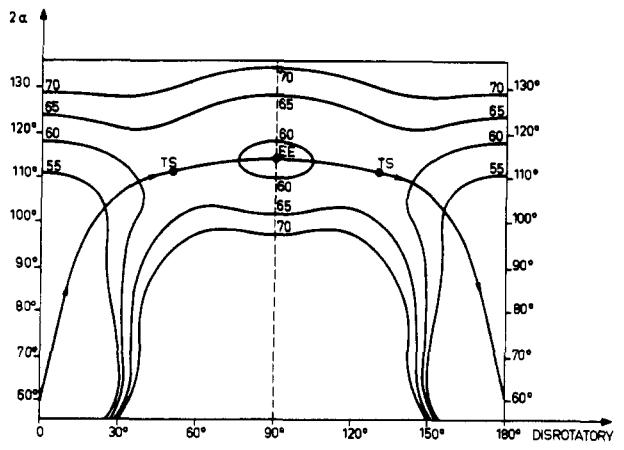

Figure 7. Two-dimensional potential energy surface and static reaction path for the synchronous disrotatory motion of the terminal methylene groups. 2α represents the value of the carbon ring angle. The abcissa gives the common absolute value of both rotational angles: $\theta = \theta_1 = -\theta_2$. TS denotes the position of a transition state. The energies are in kcal/mol.

for $2\alpha < 1.775$ rad, the rotation of a single terminal methylene group is the easiest motion; at the same time, $h_D(\alpha)$ becomes smaller than $h_C(\alpha)$.

Two-Dimensional Cuts Through $V(\alpha,\theta_1,\theta_2)$. In Figures 6, 7, and 8 are drawn in two dimensions (2α and θ) the potential isoenergetic curves obtained in the following three limiting cases: (i) synchronous conrotatory motion ($\theta_1 = \theta_2 = \theta$; cf. Figure 6); (ii) synchronous disrotatory motion ($\theta_1 = -\theta_2 = \theta$; cf. Figure 7); (iii) rotation of a single methylene group ($\theta_1 = \theta$, $\theta_2 = 0$; cf. Figure 8). These figures are just for guidance; they rely on arbitrary relationships between θ_1 and θ_2, in order to reduce the number of dimensions from three to two for clarity of the physical analysis. As a consequence, the minimum energy paths drawn in Figures 6, 7, and 8 are not necessarily absolute minimum energy paths.

However, the main feature of the overall surface appears clearly in these two-dimensional cuts: in a first step, the reaction coordinate is almost identical with a pure ring-opening motion; the rotation of the terminal groups occurs at almost constant angle ∠CCC, and finally the ring recloses and the isomer molecule is formed. The optical isomer is most easily formed via a purely conrotatory process (see Figure 6). The transition state is close to EE(α) with $2\alpha = 1.975$ rad and is energetically located at 59.8 kcal/mol above cyclopropane. In ref 2, Figure 6, it was shown that the best way to go through the transition state was the conrotatory concerted motion of both terminal groups. Consequently, in this particular case, the relationship $\theta_1 = \theta_2$, by means of which the two-dimensional surface can be visualized, does not alter at all the shape of the true reaction coordinate in the neighborhood of the transition state, in three-dimensional space.

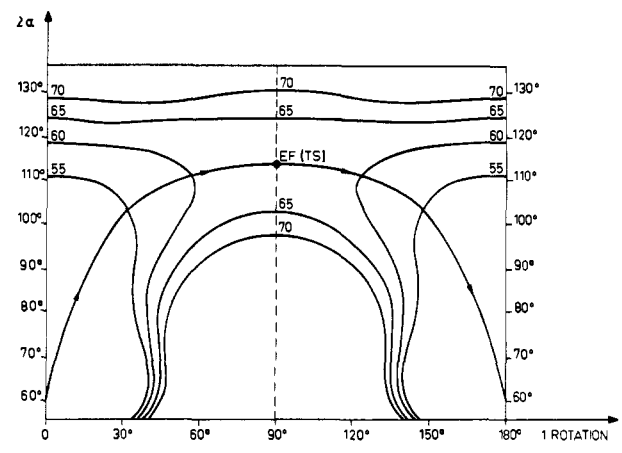

Figure 8. Two-dimensional potential energy surface and static reaction path for the rotational motion of a single terminal methylene group. 2α represents the value of the carbon ring angle. The abcissa gives the value of the rotational angle: $\theta = \theta_1$ along with $\theta_2 = 0$. TS denotes the position of a transition state. The energies are in kcal/mol.

In Figure 7, the diradical EE(α) with $2\alpha = 1.975$ rad appears to be also a secondary minimum along the synchronous disrotatory reaction path. In fact, it is not a true minimum, since a conrotatory distorsion (here, the hidden third coordinate) requires practically no activation energy. The optical isomerization via a synchronous disrotatory process requires an activation energy of 61.9 kcal/mol.

At last, the transition state for geometrical isomerization (cf. Figure 8) is the diradical EF(α) with $2\alpha = 1.975$ rad whose potential energy is 61.6 kcal/mol above that of cyclopropane. In this case, the restrictive condition $\theta_2 = 0$ imposed in drawing the two-dimensional surface causes the reaction coordinate drawn in Figure 8 to be rather different from the true reaction coordinate in three-dimensional space. This true path has indeed a noticeable component along the hidden third dimension θ_2.

It is important to remark that the potential energy valley associated with the ring-opening motion is the most narrow and the bend between this valley and the upper rotational valley is the sharpest in the case of synchronous conrotatory motion. The widening of the entrance valley and the softening of the corner is already noticeable in the case of synchronous disrotatory motion but yet more in the case of rotation of a single group. This is due to the fact that, when $2\alpha < 100°$, the three basic motions require more and more excitation energy in the order: rotation of a single group, synchronous disrotatory motion, and, last, synchronous conrotatory motion.

Numerical Fit of the Potential Energy Function. No difficulty arises for the first term of eq 6 ($V_0(\alpha)$). The SCF values are interpolated by a one-dimensional cubic spline function. For the other terms, a reparametrization is necessary for $a(\alpha)$, $b(\alpha)$, $c(\alpha)$, and $d(\alpha)$ when $2\alpha < 1.775$ rad. In this region, the fitting of eq 6, using the SCF values in Table I, does not fit closely the potential energy curves. The reparametrization is done in the following manner. First, the boundary of the attainable region is arbitrarily fixed at 70 kcal/mol above cyclopropane. The new values of the parameters are determined for the parametized curves to in-

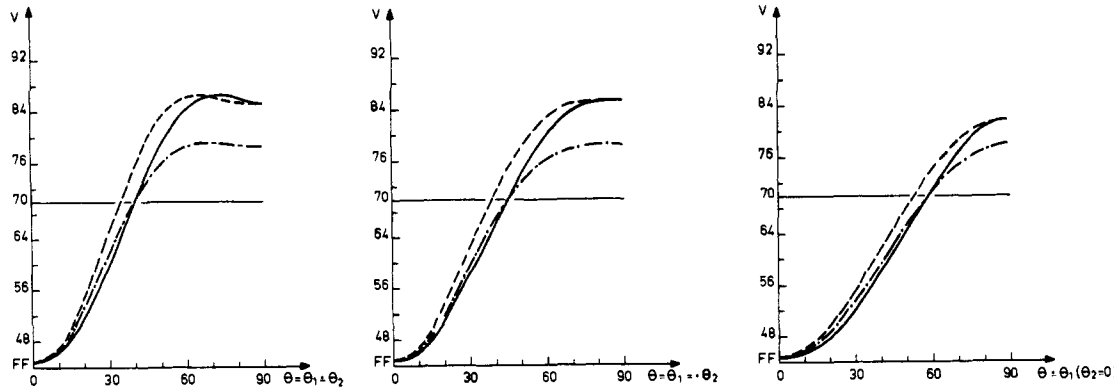

Figure 9. Potential energy curves for the three basic motions, conrotatory, disrotatory, and single rotation, respectively, at $2\alpha = 90.2°$. The energies are in kcal/mol. The curves in the solid line are SCF results. The curves in the dashed line result from eq 6 by using numerical values in Table I. Within the attainable region ($V < 70$ kcal/mol) a better fit results from using the reparametrized values of $a(\alpha)$, $d(\alpha)$, $h_C(\alpha)$, and $h_D(\alpha)$ given in Table II (dashed-dotted lines).

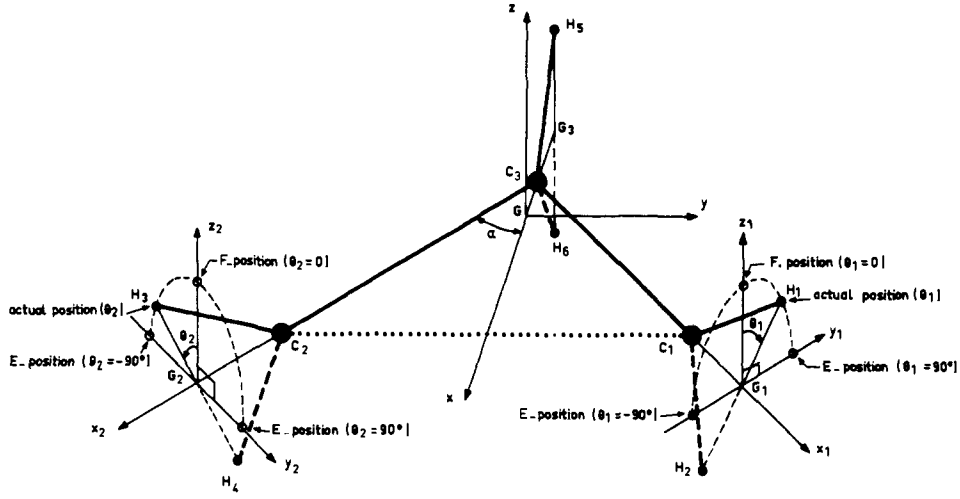

Figure 10. Definition of the dynamical variables α, θ_1, and θ_2. Particular molecular conformations are explicitly indicated.

tersect the SCF curves at $V = 70$ kcal/mol, for the three basic motions, conrotatory, disrotatory, and single rotation, respectively. The improvement is quite sensible for small values of 2α (see Figure 9). The strong energy stabilization of half-way points has no consequence for our dynamical study, since these points will never be reached. Finally, the difficulty which arose for $2\alpha < 1.275$ rad can now be ruled out. It is no longer necessary to know the energy of half-way points. Only the first part of the curves ($V < 70$ kcal/mol) need be known to get the corrected values of the parameters.

In Table II, the corrected values of $a(\alpha)$, $d(\alpha)$, $h_C(\alpha)$, and $h_D(\alpha)$ to interpolate and to insert in the fitting eq 6 are reported.

Table II. Values of EF(α), EE(α), $h_C(\alpha)$, and $h_D(\alpha)$ Used in Fitting eq 6[a]

2α, deg	$a(\alpha)$ (EF(α))	$d(\alpha)$ (EE(α))	$h_C(\alpha)$	$h_D(\alpha)$
136.1	0.25	−4.0	0	0.4
130.3	−0.3	−4.0	0	0.7
124.6	−0.5	−3.4	0	0.9
118.9	1.0	−0.4	0.7	2.6
113.2	5.2	3.2	3.4	5.5
107.4	9.3	7.9	8.1	9.2
101.7	15.4	14.8	15.1	15.4
96.0	23.6	22.9	23.7	23.4
90.2	33.3	33.6	34.6	33.6
84.5	44.5	43.5	45.9	43.5
78.8	60.3	57.8	62.9	57.8
73.1	84.0	77.8	85.9	77.8
67.3	108.1	102.5	112.2	102.5
61.6	116.8	129.5	140.7	129.5
55.9	123.4	144.1	150.8	144.1
50.1	129.4	153.1	154.6	153.1

[a] The numerical values are in kcal/mol and correspond to the energy difference between the actual conformation and that of FF(α).

Generalities for the Dynamical Study

The atomic motion driven by forces derived from the potential described in the previous section is now studied within the framework of classical mechanics.[8] A wide range of initial conditions will be covered in order to vary continuously the amount of internal energy in the molecule at the starting point of the reaction and the distribution of this energy among the different allowed motions of the molecule.

Nature of the Dynamical Model. The equations of motion in the next paragraph are established within an additional simplification, already used in ref 2. The kinetic energy of the system is written for a model in which the terminal methylene groups remain trigonal throughout the reaction (see Figure 10).

In a previous paragraph, we explained how the changes of pyramidalization of the terminal methylene groups were taken into account at the static level of the potential energy function, by means of the adiabatic function $\beta'(\alpha,\theta)$ in eq 3. Now, the very same model could be retained for the dynamical study; it would lead to terms in $\dot{\beta}_1^2$ and $\dot{\beta}_2^2$ in the expression of the kinetic energy, and also to cross terms in $\dot{\alpha}\dot{\beta}_1$, $\dot{\theta}_1\dot{\beta}_1$, $\dot{\alpha}\dot{\beta}_2$, and $\dot{\theta}_2\dot{\beta}_2$, for coupling with other modes of

distorsion of the molecule. This additional complexity makes such a model presently intractable. For this reason, we neglect the variation of β in the kinetic energy. Hence our model does not treat the changes of pyramidalization adiabatically, at the dynamical level, since the only adiabatic corrections are on the forces, not on the positions, and only indirectly on the velocities.

Equations of Motion and Initial Conditions. The present model is a simple application of the theory of constrained systems[12] in which the 3×3 A matrix is diagonal. This is due to the fact that the planes of rotation of the hydrogen atoms of the terminal CH_2 are always perpendicular to the adjacent carbon-carbon bonds, the instantaneous rotation axis. Consequently the expression of the kinetic energy is a diagonal quadratic form of the angular velocities:

$$T = \frac{1}{2} A_{\alpha\alpha}\dot{\alpha}^2 + \frac{1}{2} I(\dot{\theta}_1^2 + \dot{\theta}_2^2) \tag{10}$$

The theory of constrained system readily provides the expression of the matrix element $A_{\alpha\alpha}$ which represents the "variable mass" associated with the dynamical variable α:

$$A_{\alpha\alpha} = S \sin^2 \alpha + C \cos^2 \alpha + I(\sin^2 \theta_1 + \sin^2 \theta_2) \tag{11}$$

where

$$S = \frac{2}{M + 2m_1} \times \left\{\frac{1}{1 + 2\rho}[L(M + 2m_1) + 2m_1\lambda]^2 + M2m_1\lambda^2\right\} \tag{12}$$

$$C = 2[ML^2 + 2m_1(L + \lambda)^2] \tag{13}$$

$$I = 2m_1\mu^2 \tag{14}$$

and

$$\rho = (M + 2m_1)/(M + 2m_2) \tag{15}$$

$$\lambda = l \cos \gamma/2 \text{ and } \mu = l \sin \gamma/2 \tag{16}$$

L is the CC length, l the CH length, and γ the $\angle$HCH angle in the terminal groups, M the mass of a carbon atom, m_1 and m_2 the masses of the substituents on $C_1(C_2)$ and C_3, respectively. In the present study $m_1 = m_2 = 1$ and $\rho = 1$; I is the moment of inertia of the rotor which is formed of the two hydrogen atoms in a terminal methylene group. Equation 11 leads to the partial derivatives:

$$\partial A_{\alpha\alpha}/\partial_\alpha = (S - C) \sin 2\alpha \tag{17a}$$

$$\partial A_{\alpha\alpha}/\partial\theta_i = I \sin (2\theta_i) \qquad (i = 1, 2) \tag{17b}$$

Finally, the three Lagrangian equations of motion are:

$$\ddot{\alpha} = -\frac{1}{A_{\alpha\alpha}}\left[\frac{1}{2}\frac{\partial A_{\alpha\alpha}}{\partial\alpha}\dot{\alpha}^2 + \dot{\alpha}\left(\frac{\partial A_{\alpha\alpha}}{\partial\theta_1}\dot{\theta}_1 + \frac{\partial A_{\alpha\alpha}}{\partial\theta_2}\dot{\theta}_2\right) + \frac{\partial V}{\partial\alpha}\right] \tag{18a}$$

$$\ddot{\theta}_i = \frac{1}{I}\left[\frac{1}{2}\frac{\partial A_{\alpha\alpha}}{\partial\theta_i}\dot{\alpha}^2 - \frac{\partial V}{\partial\theta_i}\right] \qquad (i = 1, 2) \tag{18b}$$

where

$$\frac{\partial V}{\partial\alpha} = \frac{dV_0}{d\alpha} + \frac{da}{d\alpha}\sin^2(\theta_1 + \theta_2)\sin^2(\theta_1 - \theta_2) + \frac{db}{d\alpha}\sin^2(\theta_1 - \theta_2)\cos^2(\theta_1 + \theta_2) + \frac{dc}{d\alpha}\sin^2(\theta_1 + \theta_2)\cos^2(\theta_1 - \theta_2) + \frac{dd}{d\alpha}\sin^2\theta_1 \sin^2\theta_2 \tag{19a}$$

$$\frac{\partial V}{\partial\theta_i} = 2 \sin(2\theta_i)[\pm a(\alpha)\sin(\theta_1 + \theta_2)\sin(\theta_1 - \theta_2) \pm b(\alpha)\sin(\theta_1 - \theta_2)\cos(\theta_1 + \theta_2) + c(\alpha)\sin(\theta_1 + \theta_2)\cos(\theta_1 - \theta_2) + \tfrac{1}{2}d(\alpha)\sin^2\theta_{i'}] \tag{19b}$$

$$(i = 1, 2) \text{ and } (i' \neq i)$$

The + alternative should be used for $i = 1$ and the − alternative for $i = 2$, respectively.

The numerical integration of the three coupled second-order differential eq 18a and 18b requires six initial conditions. These are: (i, ii, iii) the three values $2\alpha^0$, θ_1^0, and θ_2^0, which determine the molecular geometry at the starting point (all the trajectories in the present study start with the cyclopropane molecule in its equilibrium geometry, i.e., $2\alpha^0 = 60°$, $\theta_1^0 = \theta_2^0 = 0$); (iv) the total internal energy in the molecule, E_{tot}; (v) the fraction E_{rot}^0 of initial energy attributed to the "rotations" (at starting point, this is actually vibration energy); (vi) the manner in which E_{rot}^0 is distributed among the two "rotors". This is defined by an angle (δ^0) such that:

$$tg\delta^0 = \dot{\theta}_1^0/\dot{\theta}_2^0 \tag{20}$$

where $\dot{\theta}_1^0$ and $\dot{\theta}_2^0$ are the initial rotational velocities of the two groups. Then the relationship:

$$\dot{\theta}_2^0 = \cos\delta^0[2I^{-1}E_{rot}^0]^{1/2} \tag{21}$$

is used. It is not restrictive to have $\dot{\theta}_2^0 > 0$ since $\dot{\theta}_1^0$ can be either positive or negative. A third relationship:

$$\dot{\alpha}^0 = \pm\{2[E_{tot} - E_{rot}^0 - V(\alpha^0,\theta_1^0,\theta_2^0)]/A_{\alpha\alpha}(\alpha^0,\theta_1^0,\theta_2^0)\}^{1/2} \tag{22}$$

is necessary to define the initial $\angle$CCC angular velocity. The present study has been arbitrarily limited to $\dot{\alpha}^0 > 0$, i.e., to initial extensions of the CC bond.

Five different values of E_{tot} have been studied, namely 61, 62, 63, 64, and 65 kcal/mol. For E_{tot} = 61 kcal/mol, the only available channel is the synchronous conrotatory motion (transition state at 59.8 kcal/mol). For $E_{tot} \geq 62$ kcal/mol, the rotation of a single group (transition state at 61.6 kcal/mol) and the concerted disrotatory motion (transition state at 61.9 kcal/mol) both become feasible motions, at least in principle. For each value of E_{tot}, E_{rot}^0 has been varied stepwisely from 2 to 50 kcal/mol, with a step of 2 kcal/mol. In addition, for given values of E_{tot} and E_{rot}^0, δ^0 has been varied from 45° (conrotatory motion, i.e., antisymmetric vibration of the methylene groups) to −45° (disrotatory motion, i.e., symmetric vibration), with a step of 10°. All things considered, about 1500 trajectories have been run.[13]

In our model, no fraction of the total energy in the molecule can be transferred to nonreactive intramolecular modes, nor can any fraction be exchanged with the medium. Under this assumption, the computed trajectories are endless; a given set of initial conditions leads to an infinite sequence of ring openings, rotations, and ring closures. The integration of a trajectory is stopped the first time the representative point of the molecule moving on the surface enters a prescribed narrow region around the absolute minimum, i.e., the representative point of cyclopropane in its equilibrum geometry. This is consistent with the analysis of the reaction given by Doering and Sachdev within the RRK model.[14] Their conclusion was that "the best trap for a diradical is its own reclosure to a covalent bond", because there the energy "is rapidly dissipated by distribution among other, nonreactive modes. The larger the number of atoms . . . in the molecule, the more nearly true this statement is".

Dynamical Results

We first treat separately the trajectories corresponding to

the particular values $\delta^0 = 45$ and $-45°$. Indeed the total symmetry of the problem is such that, whenever the motion of both rotors at the starting point is either purely conrotatory or purely disrotatory, it keeps this particularity throughout the trajectory. Then, the trajectory can be drawn on a two-dimensional potential energy surface such as that pictured in Figures 6 and 7.

Synchronous Conrotatory Motion ($\delta^0 = 45°$). For a very weak amount of excess energy (1.2 kcal/mol) with respect to the conrotatory transition state (59.8 kcal/mol), a rather striking phenomenon occurs: reactive trajectories are observed only when E_{rot}^0 (initial "rotational" energy here exclusively in the antisymmetric twisting vibration of the methylene groups) lies between 30.4 and 32.4 kcal/mol (see Figure 11). Thus, in order to observe the optical isomer formed in a purely conrotatory fashion, one half of the total molecular internal energy must be placed in the methylene groups. The other half of the total energy (28.6 to 30.6 kcal/mol) remains in the stretching vibrational mode of the carbon-carbon bond. At first sight, this would seem insufficient to bring about the opening of the carbon ring. However, during the first part of the reaction (from point A to point B in Figure 11), the ring-opening motion and a complete oscillation of both terminal groups (with an amplitude of 20°) go on simultaneously. Hence an important energy transfer occurs from the methylene groups to the carbon-carbon bond. Then only, the carbon ring can open. Afterwards, the methylene groups rotate by 180° (from B to C in Figure 11); in the mean time, the value of the ∠CCC angle oscillates weakly around the optimum value 113°. The reaction ends with a motion of ring closure (from C to D in Figure 11).

When the total intramolecular energy increases ($E_{tot} \geq$ 62 kcal/mol), the reactive trajectories are more numerous. Below, we analyze in detail the set of trajectories for $E_{tot} =$ 62 kcal/mol (see Figure 12). Depending on the value of E_{rot}^0, several distinguishable motions are observed.

$E_{rot}^0 \leq$ 10 kcal/mol. The trajectories are nonreactive. As shown in Figure 12a, the carbon ring opens and recloses without reaching the transition state. This is simply due to a lack of twisting energy in the methylene groups at the starting point.

12 kcal/mol $\leq E_{rot}^0 \leq$ 20 kcal/mol. Within these limits the trajectories are reactive (see Figures 12b-d). They are quite different from the trajectory in Figure 11; only one-half of an oscillation of the methylene groups occurs during the ring-opening phase. In Figure 12b the first reactive trajectory of this type is pictured; during the rotation of the methylene groups, the carbon ring angle oscillates many times around the optimum value 113° and, consequently, the duration of the phase of rotation is long (3.3×10^{-13} sec). This means that the way in which the representative point reaches the upper valley is far from being ideal. The ideal situation occurs when $E_{rot}^0 = 16$ kcal/mol (see Figure 12c); then, the methylene groups rotate very easily in 2.2×10^{-13} sec. Finally, for $E_{rot}^0 \simeq 20$ kcal/mol (see Figure 12d) the rotational process is again difficult and lengthy (4.4×10^{-13} sec). It is quite important to note that all these trajectories include only a *single rotation of 180°* by each terminal group. This result is all the more surprising since the energy in the rotational motion can only be transferred, in our model, to the vibration of the carbon-carbon bond, and not to a nonreactive mode.

22 kcal/mol $\leq E_{rot}^0 \leq$ 32 kcal/mol. The trajectories are nonreactive, as pictured in Figures 12e and 12f. When the ring opens, the energy is badly distributed among the different possible modes and the transition state cannot be reached. In Figure 12e, the representative point, after a half oscillation of the methylene groups, bounces off the edge of the lower potential energy bump toward the upper part of the figure. In Figure 12f, the same thing occurs, but after a complete oscillation.

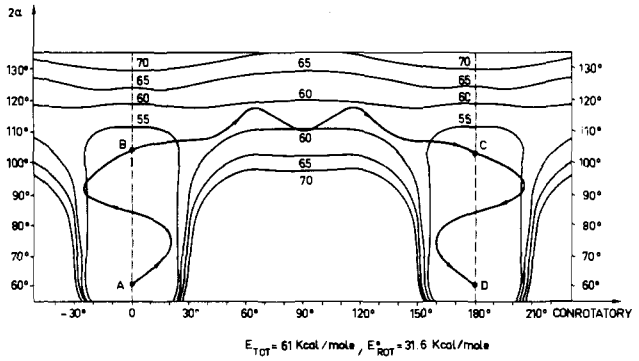

Figure 11. A low total energy (61 kcal/mol) reactive trajectory leading from cyclopropane to the optical isomer via a purely conrotatory process ($\delta^0 = 45°$).

32.4 kcal/mol $\leq E_{rot}^0 \leq$ 35.2 kcal/mol. Within these limits, the trajectories are again reactive (see Figure 12g) and of the same type as that pictured in Figure 11. As previously, each terminal group rotates by only 180°. It should be emphasized that this second "reactive band" of initial rotational energies is much more narrow than the first one. This can be explained as follows: the rotations occur after a complete oscillation of the methylene groups. This first part of the reaction (ring opening) lasts longer in the trajectories of the second band (32.4 to 35.2 kcal/mol) than in the trajectories of the first "reactive band" (12 to 20 kcal/mol). Therefore the reactive trajectories are much more "focused" around the ideal trajectory; a slight modification can lead to large deviations and rapidly to nonreactive trajectories.

$E_{rot}^0 \geq$ 36 kcal/mol. These trajectories are nonreactive (see Figure 12h). The energy initially concentrated into the stretching mode of the carbon-carbon bond is too small ($\leq$26 kcal/mol) to allow a sufficient opening of the carbon ring.

For total intramolecular energies greater than 62 kcal/mol ($E_{tot} =$ 63, 64, 65 kcal/mol), the two "reactive bands" of initial E_{rot}^0 values still exist (see Figure 13a) and even become larger and larger with increasing E_{tot}. This is due to the fact that, the greater the excess energy, the easier it is for the representative point of the molecule to step over the transition state, even if the approach coordinate is not favorable. Moreover, the second reactive band shifts slightly toward higher values of E_{rot}^0, so that the first phase of the reaction (ring opening along with a complete oscillation of the methylene groups) always results in a face-to-face diradical with a ∠CCC angle close to 105°.[15]

At this stage, we can formulate three statements. (i) There exist two well-defined bands in E_{rot}^0, within which reactive trajectories obtain.[16,17] (ii) The great majority of reactive trajectories (40 out of 44) lead to only a single concerted rotation by 180° of the terminal groups. This is in good agreement with the analysis of the reaction given, on the basis of the RRK model, in ref 14, as well as with experimental works on the deactivation of the rotational modes.[18] (iii) The initial "rotational" (vibrational) energy required for reaction is much larger than what was estimated on the basis of static information.

We now turn to an interpretation of these results by looking back at the two-dimensional potential energy surface for synchronous conrotatory motion. This surface has a symmetry axis ($\theta = 90°$) (Figure 6). The transition states correspond to rotation angles of 58 and 122°, respectively,

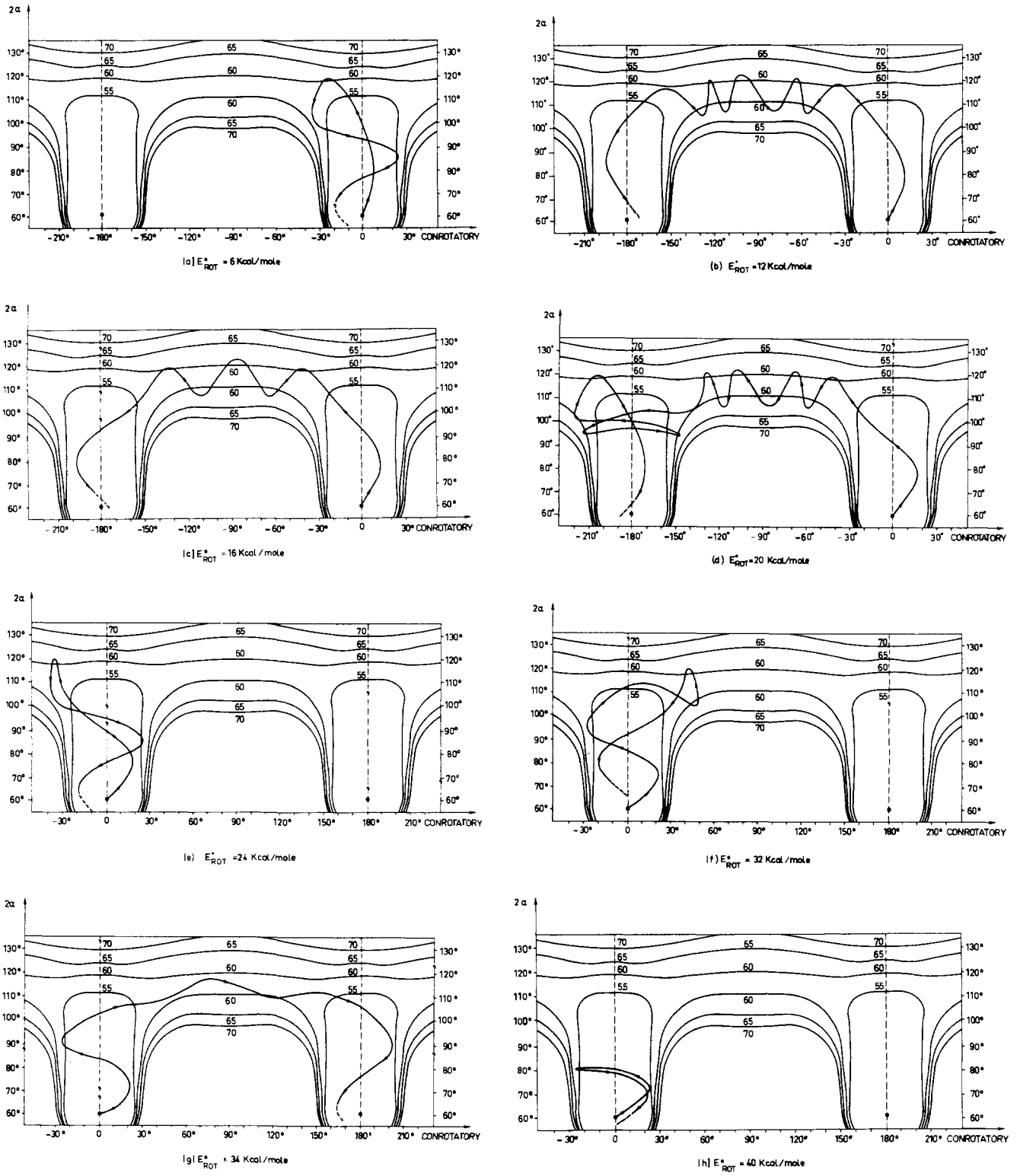

Figure 12. Typical conrotatory trajectories at E_{101} = 62 kcal/mol for different initial "rotational" (vibrational) energies.

the ring angle being then close to the value 113°. It is interesting to compare this surface with the two different types of parametrized surfaces that were used to study the dynamical properties of the exchange reactions A + BC → AB + C.[19] These two surfaces differed by the position of the potential energy barriers, located either in the entrance valley or in the exit valley. Considered as a whole, the potential energy surface driving the conrotatory isomerizations involves in fact three valleys: the first valley drives the ring-opening motion; in the second valley, the rotations of the terminal groups occur; the third valley is that of the ring reclosure. Strictly speaking, it is therefore improper to discriminate, in the present case, between the two possibilities of the transition state being located either in the entrance valley or in the exit valley, because everything is symmetric. However, since reaching the edge-to-edge half-way point EE most often brings completion of the reaction, we consider the valley of ring opening as the "entrance" valley and the upper valley of rotation (FF → EE) as the "exit" valley, which therefore includes the transition state. Qualitatively, the partial energy helping initially to break the carbon-carbon bond and the initial "conrotatory rotation" (antisym-

metric vibration) energy in the methylene groups play the same roles as respectively the translation and vibration energies in those exchange reactions A + BC → AB + C for which the transition state lies in the exit valley. Thus, similar effects can be invoked in both cases to explain why a rather large amount of "vibrational" energy is required for the trajectories to be reactive: (i) the valley corner must be cut close by the representative point to avoid bouncing off on the lateral potential energy walls, and this is possible only when vibration (here methylene oscillation) transforms into translation (here CC stretch); (ii) centrifugal effects forbid a proper energy transfer from translation (CC stretch) to vibration (methylene oscillation) when the initial translation energy (CC stretch energy) is too great. It should be kept in mind that the first "reactive band" to appear as the total energy increases is that for very high "rotation" (vibration) energies ($E_{rot}^0 \simeq 32$ kcal/mol). The exact threshold is $E_{tot} = 60.4$ kcal/mol. The threshold for the other reactive band ($E_{rot}^0 \simeq 12$ to 20 kcal/mol) is $E_{tot} = 61.4$ kcal/mol (see Figure 13a).

The results presented in this section all depend strongly on the assumption which allowed us to terminate the trajectories. For instance, certain "reactive" trajectories, if they were free to go on, could come back to the starting point of the reaction. Conversely, certain "nonreactive" trajectories, after the first process of ring opening and closure, could yield a cyclopropane molecule possessing a more suitable amount of CH_2 vibration energy and the isomerization reaction could now be possible (Figure 12a). Furthermore, the treatment of the dynamical problem in its *full dimensionality* might well make the unreactive region between the two reactive bands disappear.

Synchronous Disrotatory Motion ($\delta^0 = -45°$). The main results of the previous section for conrotatory trajectories remain true in the case of disrotatory trajectories. According to the value of E_{rot}^0 (here the initial CH_2 symmetric vibration energy), two reactive bands are still observed and exhibit the same characteristics as above: the first band corresponds to values of E_{rot}^0 of the order of 20 kcal/mol and the second band to values of E_{rot}^0 of the order of 40 kcal/mol. Most of the reactive trajectories involve a single concerted rotation of the terminal groups.

The only noticeable difference concerns the nature of the reactive trajectories when the total energy is only weakly in excess of that of the transition state. For the lowest total intramolecular energy studied ($E_{tot} = 63$ kcal/mol, i.e., $E_{tot} - E_{TS} = 1.1$ kcal/mol), we observe reactive trajectories in the first band only, i.e., for E_{rot}^0 lying between 16 and 26 kcal/mol. This is exactly opposite to what happens in the case of a synchronous conrotatory motion at $E_{tot} = 61$ kcal/mol ($E_{tot} - E_{TS} = 1.2$ kcal/mol) where reactive trajectories are observed in the second band only. The difference is probably due to the disrotatory transition state lying closer to the entrance valley than the conrotatory transition state (the top of the rotational barrier is at $\theta_1 = -\theta_2 = 50°$ presently, instead of $\theta_1 = \theta_2 = 58°$ before). Moreover, the entrance valley which drives the ring opening is wider in the disrotatory case than in the conrotatory case because disrotatory distorsions require a smaller amount of energy than conrotatory distorsion, as long as $2\alpha < 95°$.

More precise calculations indicate that the first reactive band appears at $E_{tot} = 62.1$ kcal/mol and the second reactive band at $E_{tot} = 63.1$ kcal/mol. The evolution of the reactive band widths versus the total energy is represented in Figure 13b.

The small secondary minimum (well depth: 2.3 kcal/mol) at the edge-to-edge half-way point does not affect the trajectories very much even for the lowest total energy. However, there are some rare exceptions where the representative point of the molecule spends a rather long time in this region of the potential energy surface (for certain trajectories, the integration was stopped after 1.5 10^{-12} sec and the molecule was still trapped into the well). Then, the final outcome of the reaction is quite a random phenomenon.

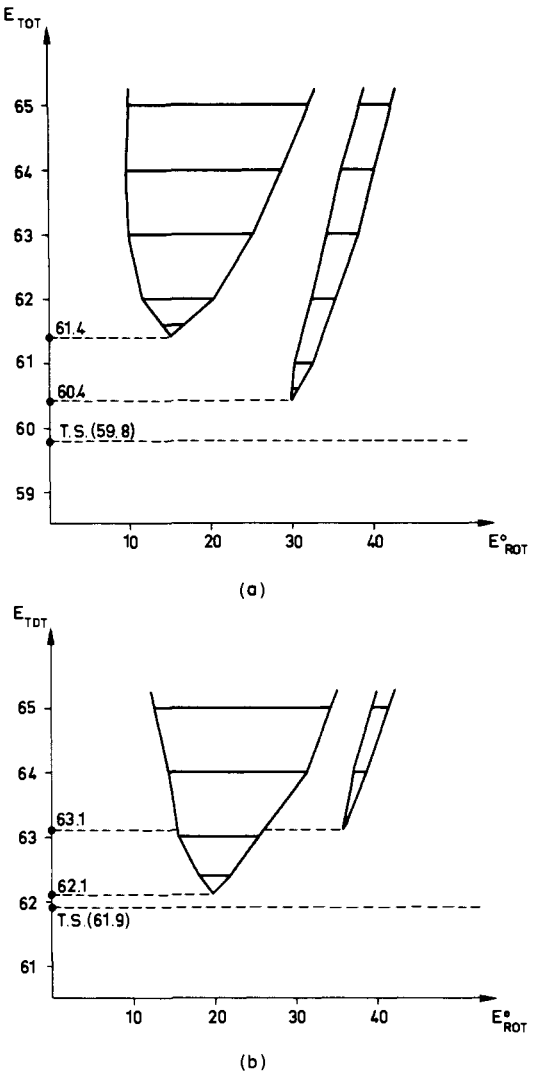

Figure 13. Evolution of the "reactive bands" versus E_{tot} and E_{rot}^0 for (a) a conrotatory motion of the terminal groups and (b) a disrotatory motion.

General Motion (General δ^0). When δ^0 differs from ±45°, the coupling between the rotations of both methylene groups results, at anytime, in an energy transfer from one to the other. Then the first question arises: for a given value of δ^0 characterizing the distribution of the initial methylene "rotation" (vibration[20]) energy, what is the actual value of $\delta = tg^{-1}(\dot{\theta}_1/\dot{\theta}_2)$ after the ring-opening phase of the reaction is terminated?

In ref 2, we noted that the process of ring opening is much faster than the rotations of the terminal groups whatever the type of cyclopropane molecules, either substituted or not. Consequently, energy transfer between the two oscillating terminal groups does not have time to operate significantly while the carbon ring opens. The opened molecule is rather similar to FF-type diradical whose CH_2 rotational energy, which is possibly very different from E_{rot}^0, is nevertheless distributed among both rotors in almost the same way as that defined by δ^0 at the starting point. A careful study of the relative variations with time of θ_1 and θ_2 leads to the following conclusion. Whatever the value of δ^0, the corresponding trajectory, when reactive, closely resembles

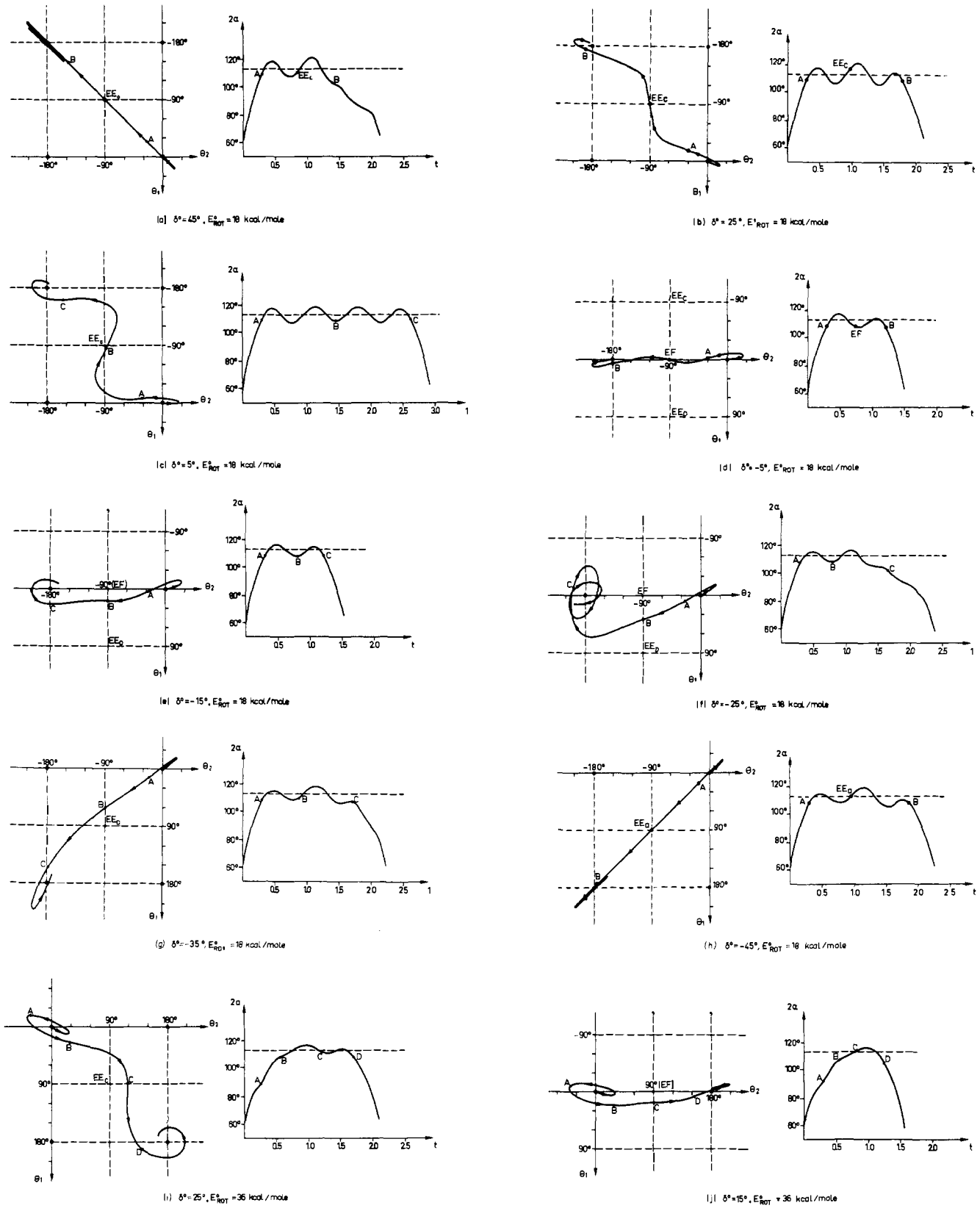

Figure 14. Typical trajectories at E_{tot} = 63 kcal/mol and either E_{rot}^0 = 18 kcal/mol (a to h) or E_{rot}^0 = 36 kcal/mol (i and j), for different values of δ^0. The part in θ_1 and θ_2 of each trajectory is pictured on the left side; on the right side, the evolution of the carbon ring angle versus time is represented. The time unit is here 10^{-13} sec.

the reactive trajectory obtained for the same value of δ^0 on the rotational potential energy surface at *constant* ∠CCC angle (see ref 2, Figure 7). Thus, if $\delta^0 > 0$, the rotation of the terminal groups most often leads, via a conrotatory process, to a molecular configuration close to that of an edge-to-edge diradical (EE_C). If $\delta^0 < 0$, we observe either the rotation of a single terminal group (EF), or within a narrow range close to −45°, the formation via a disrotatory process of an edge-to-edge diradical (EE_D). It should be emphasized that, whatever the value of δ^0, both reactive bands (corresponding to values of E_{rot}^0 of the order of 20 and 40 kcal/mol, respectively) are still observed.

(a) Typical Trajectories at E_{tot} = 63 kcal/mol (E_{rot}^0 = 18 and 36 kcal/mol). The particular value 63 kcal/mol of the total energy has been selected because it should allow passage over any of the transition states. We also select initial "rotation" (vibration) energy values of 18 and 36 kcal/mol because, whatever δ^0, they fall into the first and second "reactive bands", respectively. In Figure 14, the variation of θ_1 and θ_2 on the one hand, and that of the ring angle ∠CCC with time on the other hand, are pictured side by side for different values of δ^0. Particular points (A, B, ...) are indicated on both curves which show clearly that rotation of the terminal groups leading to formation of isomer molecules occurs when the ring angle is opened and keeps an almost constant value close to 113°.

The following discussion on the nature of the reaction product is valid only under the *assumption* that in the reactant cyclopropane molecule, only one carbon-carbon bond can break. Then, a concerted rotation of 180° (either conrotatory or disrotatory) of both terminal groups leads to the optical isomer whereas the rotation of a single group leads to the geometrical isomer.[21]

Reactive Trajectories of the First Type (E_{rot}^0 = 18 kcal/mol). For δ^0 = 45°, there is no possible energy transfer between the two rotating groups. In the referential (θ_1,θ_2), the trajectory is therefore linear (see Figure 14a) and goes exactly through the representative point of the molecular configuration EE_C. The optical isomer is obviously formed.

When δ^0 is different from 45°, the trajectory deviates more or less with respect to this optimal path (see Figures 14b and 14c). It is observed that, as mentioned previously, (i) the distribution of energy among the two rotors once the ring is opened (point A) is hardly different from the initial distribution defined by δ^0 and (ii) the greatest part of the rotational motion (from A to B in Figure 14b, and A to C in Figure 14c) occurs when the ring is opened. In the rotational phase of the reaction, which is crucial for the result of the reaction, the molecule is therefore sensitive to the disrotatory potential energy barriers, and tends to fall back into the conrotatory valley. In the part of the trajectory close to EE_C, a single group rotates significantly (locally δ = 85°) when initially δ^0 = 25° (see Figure 14b), whereas both groups rotate almost disrotatorily (locally δ = −63°) when initially δ^0 = 5° (see Figure 14c). This trajectory is precisely the last one, as δ^0 tends toward negative values, to produce the optical isomer as product of the reaction. The poor initial distribution of "rotation" (vibration) energy causes an important lengthening of the time required for the rotations to take place. Three and a half full vibrations of the carbon ring angle around its local equilibrium value (113°) have time to occur. Finally, it is important to remark that the part in θ_1,θ_2 of this trajectory has quite the same shape as the two-dimensional trajectory presented in ref 2, Figure 7b, for a very similar value of δ^0 (4°).

Within the range $-5° \geq \delta^0 > -35°$, the trajectories lead to formation of the geometrical isomer (see Figures 14d-f). The trajectory corresponding to δ^0 = −5° (Figure 14d) goes exactly through the representative point of the configuration EF, along with a rather conrotatory local motion (δ = 17°). When δ^0 becomes more and more negative, the point B at which the trajectories cut the axis θ_2 = −90° becomes progressively closer and closer to the half-way point of the synchronous disrotatory motion (molecular configuration EE_D).

When δ^0 is close to −45°, the optical isomer is formed via a disrotatory process (see Figures 14g and 14h).

Reactive Trajectories of the Second Type (E_{rot}^0 = 36 kcal/mol). Figures 14i and 14j illustrate two particular reactive trajectories of the second type. The first one leads to optical isomerization (δ^0 = 25°, cf. Figure 14i) and the second one leads to geometrical isomerization (δ^0 = 15°, cf. Figure 14j). The complete vibration of both methylene groups during the ring-opening phase of the reaction is readily observed in relative variations with time of the angles θ_1 and θ_2. Moreover, in the second diagrams of each figure, showing how the carbon ring angle varies in the course of the reaction, it is observed that the phase of ring opening is longer in the reactive trajectories of this second type than in those of the first type.

(b) Nature of the Reaction Product as a Function of E_{tot}, E_{rot}^0, and δ^0. Tables III, IV, and V recapitulate the results of the trajectories for the following values of the total energies: 62, 63, and 64 kcal/mol.[22] For reactive trajectories, the nature of the half-way point is specified. In most cases, a maximum of one rotation occurs for either CH_2 group in the opened diradical so that the nature of the product of the reaction is easily deducible from the nature of the half-way point, according to the following correspondence scheme:

$$EE_C \text{ and } EE_D \rightarrow \text{optical isomer} \quad \text{(i)}$$

$$EF \rightarrow \text{geometrical isomer} \quad \text{(ii)}$$

When several rotations follow one another before the carbon ring recloses, the nature of the isomer formed depends on the particular case; it is specified in Tables III, IV, and V.

E_{tot} = 62 kcal/mol (cf. Table III). The optical isomer is exclusively formed (via EE_C). The amount of excess energy above the potential energy of transition state is weak (2.2 kcal/mol), so that it is only within the range $\delta^0 \geq 25°$, i.e., close to the optimal value δ^0 = 45°, that the reaction is possible. In all the reactive trajectories studied, the ring reclosure occurs after only a single concerted 180° rotation of the terminal groups.

E_{tot} = 63 kcal/mol (cf. Table IV). The total energy is now sufficient for the three distinct rotational processes within the diradical species to be possible. When δ^0 varies from 45° to −45°, we observe successively the formation of the optical isomer via conrotatory process, then the geometrical isomer, and last the optical isomer via disrotatory process. Reactive trajectories involving several rotations of the terminal groups within the diradical appear. They correspond, most often, either to limits (on the reactive side) between "reactive" and "nonreactive" bands, or, within a reactive band, to limiting values of δ^0 and E_{rot}^0 beyond which there is a change in the nature of the isomer formed.

E_{tot} = 64 kcal/mol (cf. Table V). The excess energy over and above the potential energy of the transition states increases and, thus, the reactive bands become wider.

Concluding Remarks

The dynamical study of the coupling between the modes of ring opening (and closure) and the modes of rotation of the methylene groups of a cyclopropane molecule in the course of isomerization reactions confirms essentially the conclusions of the static study.[6] An isomerization involves, at least approximately, three sequential steps: ring opening, methylene rotation (s), and ring closure. Moreover, one of the results of our previous simplified dynamical study is also corroborated; the relative motion of the terminal groups, during the phase of rotation within the diradical, depends strongly on the initial conditions.

The main conclusions of the present dynamical study are: (i) the amount of initial methylene "rotation" (vibration) energy required for the reaction to be possible is much larger than was previously estimated; two reactive bands (12-24 kcal/mol and 34-36 kcal/mol approximately) always appear which correspond to two different reaction mechanisms; (ii) in general, a single rotation of 180° of one or

Table III. Nature of the Half-Way Point for Reactive Trajectories, Depending on the Values of δ^0 and $E_{rot}{}^0$, when E_{tot} = 62 kcal/mol[a]

	$E_{rot}{}^0$																								
δ^0, deg	2	4	6	8	10	12	14	16	18	20	22	24	26	28	30	32	34	36	38	40	42	44	46	48	50
−45																									
−35																									
−25																									
−15																									
−5																									
5																									
15																									
25							EE_C	EE_C	EE_C								EE_C								
35						EE_C	EE_C	EE_C	EE_C	EE_C		EE_C					EE_C								
45						EE_C	EEC	EE_C	EE_C	EE_C							EE_C								

[a] The blank terms of the array correspond to nonreactive trajectories.

Table IV. Nature of the Half-Way Point, Depending on the Values of δ^0 and $E_{rot}{}^0$, when E_{tot} = 63 kcal/mol[a]

	$E_{rot}{}^0$																								
δ^0, deg	2	4	6	8	10	12	14	16	18	20	22	24	26	28	30	32	34	36	38	40	42	44	46	48	50
−45								EE_D	EE_D	EE_D	EE_D	EE_D	EE_D												
−35								EE_D	EE_D	EE_D	EE_D	EE_D	EE_D												
−25								EF	EF	$EF^{(1)}$	$EE_D{}^{(1)}$	EE_D	EE_D				EF	EF							
−15								EF	EF	EF	EF	EF	EE_D					$EF^{(2)}$							
−5								$EF^{(2)}$	EF	EF	EF	EF						EE_D	$EF^{(2)}$						
5								EE_C	EE_C	EF	EF							EF	EE_D						
15							$EE_C{}^{(1)}$	EE_C	EE_C	EE_C	EE_C							EF	EF						
25						EE_C	EE_C	EE_C	EE_C	EE_C	EE_C							EE_C							
35						EE_C	EE_C		EE_C		EE_C	EE_C	EE_C					EE_C							
45					EE_C	EE_C	EE_C		EE_C	EE_C		EE_C						EE_C	EE_C						

[a] The blank terms of the array correspond to nonreactive trajectories. Several rotations within the diradical lead either to the starting molecule (1) or to the geometrical isomer (2).

Table V. Nature of the Half-Way Point, Depending on the Values of δ^0 and $E_{rot}{}^0$, when E_{tot} = 64 kcal/mol[a]

	$E_{rot}{}^0$																								
δ^0, deg	2	4	6	8	10	12	14	16	18	20	22	24	26	28	30	32	34	36	38	40	42	44	46	48	50
−45								EE_D	EE_D	EE_D	EE_D	EE_D	EE_D	EE_D	EE_D				EE_D						
35								EE_D	EE_D	EE_D	EE_D	EE_D	EE_D	EE_D	EE_D				EE_D						
25								EF	EF	$EF^{(1)}$	$EF^{(2)}$	$EE_D{}^{(1)}$	EE_D	EE_D	EE_D				EE_D	EF					
−15							EF	EF	EF	$EF^{(2)}$	EE_D	EE_D	$EE_D{}^{(2)}$	EE_D					EE_D						
−5							EF	EF	EF	EF	EF	EF	$EF^{(1)}$	EF					$EF^{(1)}$	EE_D					
5				EE_C	EE_C	EF	$EF^{(2)}$	EF	EF	EF	EF	EF	$EF^{(1)}$	EF					EF						
15						EE_C	EE_C	EE_C	EE_C	EE_C	EE_D	EF	EF						EF						
25				EE_C		EE_C		EE_C	EE_C	EE_C	EE_C	EE_C	EE_C						EE_C						
35					$EE_C{}^{(1)}$	EE_C	$EE_C{}^{(1)}$	EE_C	EE_C	EE_C	EE_C	EE_C	EE_C	EE_C						EE_C	EE_C					
45					EE_C	$EE_C{}^{(1)}$	EE_C	EE_C	EE_C	EE_C	EE_C	EE_C	EE_C	EE_C					EE_C	EE_C						

[a] The blank terms of the array correspond to nonreactive trajectories. Several rotations within the diradical lead either to the starting molecule (1), or the geometrical isomer (2), or to the optical isomer (3).

both terminal groups occurs within the diradical species; (iii) the majority of the reactive trajectories lead, especially at low total intramolecular energies, to formation of the optical isomer, via the half-way point EE. This result can be simply explained on the basis of the static potential energy surface; the activation energy required to reach the coplanar diradical (EE) is lower than that required to reach the orthogonal diradical (EF). No dynamical factor tends to inverse the preference for the minimum energy path over any other path. This conclusion is in good agreement with recent experimental tests of the relative rates of optical and geometrical isomerizations in optically active *trans*-cyclopropane-*1,2-d*$_2$ and 1-phenylcyclopropane-*2-d*.[23] The kinetic analysis of these reactions is consistent with a mechanism involving exclusive synchronous rotation of two methylene groups.

In connection with the experimental estimates of the relative rates of rotations and C-C cleavage in three- and four-membered rings,[24] we are presently studying the influence of heavy substituent groups on the dynamical coupling between the ring opening (or closure) and the rotations of the terminal groups.

Acknowledgment. Professor Lionel Salem's very helpful contributions to the present study are gratefully acknowledged.

References and Notes

(1) The Laboratoire de Chimie Théorique is also associated with the C.N.R.S.
(2) Y. Jean and X. Chapuisat, *J. Am. Chem. Soc.*, **96**, 6911 (1974).
(3) (a) W. J. Hehre, R. F. Stewart, and J. A. Pople, *J. Chem. Phys.*, **51**, 2657 (1969); (b) G. A. Segal, *J. Am. Chem. Soc.*, **96**, 7892 (1974).
(4) R. M. Stevens, *J. Chem. Phys.*, **52**, 1397 (1970).
(5) The values in parentheses are those obtained in a previous static study (cf. ref. 6).
(6) Y. Jean, L. Salem, J. S. Wright, J. A. Horsley, C. Moser, and R. M. Stevens, *Pure Appl. Chem., Suppl.*, **1**, 197 (1971).
(7) R. Hoffmann, *J. Am. Chem. Soc.*, **90**, 1475 (1968).
(8) For the nuclear motion in the field of the electrons, classical mechanics does not reproduce purely quantum mechanical effects, such as tunnel transmission and over barrier reflection [cf. ref 9]. However, it is known from various semiclassical studies on molecular systems of a highly quantum mechanical nature (collinear H + H_2 → H_2 + H exchange reaction for instance) that classical mechanics describes correctly nuclear rearrangement processes [cf. ref 10]. Furthermore, previous trajectory works on unimolecular reactions were undertaken within the framework of classical mechanics [cf. ref 11].
(9) G. Wolken and M. Karplus, *J. Chem. Phys.*, **60**, 351 (1974); D. J. Diestler and M. Karplus, *ibid.*, **55**, 5832 (1971); K. P. Fong and D. J. Diestler, *ibid.*, **56**, 3200 (1972); J. M. Bowman and A. Kuppermann, *Chem. Phys. Lett.*, **12**, 1 (1971).
(10) W. H. Miller, *Acc. Chem. Res.*, **4**, 161 (1971); W. H. Miller, *Adv. Chem. Phys.*, **25**, 69 (1974).
(11) H. H. Harris and D. L. Bunker, *Chem. Phys. Lett.*, **11**, 433 (1971); D. L. Bunker and W. L. Hase, *J. Chem. Phys.*, **59**, 4621 (1973); D. L. Bunker, *ibid.*, **40**, 1946 (1964); D. L. Bunker and M. T. Pattengill, *ibid.*, **48**, 772 (1968).
(12) X. Chapuisat and Y. Jean, to be published.
(13) The time reversibility and conservation of the total energy were verified every time we looked for them explicitly. No failure was diagnosed by the program test when running a trajectory.
(14) W. Von E. Doering and K. Sachdev, *J. Am. Chem. Soc.*, **96**, 1168 (1974).
(15) Third and fourth reactive bands are also observed. They correspond to, respectively, 1.5 and 2 oscillations of the methylene groups during the ring-opening process. They are quite narrow and located at 1 and 2 kcal/mol, respectively (for E_{tot} = 65 kcal/mol), above the second reactive band. Since $E_{tot}{}^0$ is scanned with quite a large step compared with the widths of these bands, very few trajectories within these bands were run.
(16) A long time ago, F. T. Wall and R. N. Porter, *J. Chem. Phys.*, **39**, 3112 (1963), mentioned the existence of upper energy bounds for H + H_2 collinear reactions. More recently, Wright et al. have observed reactive and unreactive "bands", quite similar to that in the present article, for exchange reactions resulting from collinear atom-molecule collisions: J. S. Wright, G. Tan, K. J. Laidler, and J. E. Hulse, *Chem. Phys. Lett.*, **30**, 200 (1975).
(17) The boundaries of these two bands depend partly on the curvature of the potential energy surface within a narrow region surrounding the absolute minimum (equilibrium cyclopropane). The poor description of the force constants, by quantum mechanical calculations using a minimal basis set, thus is a possible source of errors.
(18) R. A. Newark and C. H. Sederholm, *J. Chem. Phys.*, **43**, 602 (1965).
(19) J. C. Polanyi and W. H. Wong, *J. Chem. Phys.*, **51**, 1439, 1451 (1969).
(20) Now, the initial vibrational motion follows from the superposition of normal symmetric and antisymmetric motions of the two methylene groups.
(21) At the present time, the assumption that only the substituted bond breaks in the course of the isomerization is not experimentally confirmed. In particular when the substitution groups are replaced by deuterium atoms, the three bonds of the carbon ring can break equally. Then conrotatory and disrotatory concerted motions produce also the geometrical isomer.
(22) At E_{tot} = 61 kcal/mol, we studied only the trajectories relative to δ^0 = 45° because the excess energy in the molecule is so weak as to lead to nonreactive trajectories for other values of δ^0.
(23) J. A. Berson and L. D. Pedersen, *J. Am. Chem. Soc.*, **97**, 238 (1975); J. A. Berson, L. D. Pedersen, and B. K. Carpenter, *ibid.*, **97**, 240 (1975).
(24) R. J. Crawford and T. R. Lynch, *Can. J. Chem.*, **46**, 1457 (1968); J. A. Berson and J. M. Balquist, *J. Am. Chem. Soc.*, **90**, 7343 (1968); R. G. Bergman, *ibid.*, **90**, 7344 (1968); R. G. Bergman and W. L. Carter, *ibid.*, **91**, 7411 (1969); J. A. Berson, D. C. Tompkins, and G. Jones, *ibid.*, **92**, 5799 (1970).

Theoretical Studies of the Protonation of Cyclobutane

Tapani Pakkanen* and J. L. Whitten

Contribution from the Department of Chemistry, State University of New York at Stony Brook, Stony Brook, New York 11794. *Received April 28, 1975*

Abstract: The protonation of cyclobutane has been studied theoretically using ab initio methods. The protonation energy is found to be quite large, 126 kcal/mol, but is significantly lower than obtained for the protonation of cyclopropane by similar theoretical calculations. The protonation energies for edge and corner protonation of cyclobutane were found to be essentially identical.

The relative stabilities of protonated cycloalkanes have been a subject of recent experimental and theoretical studies.[1-7] These compounds have been postulated to be intermediates in acid-catalyzed reactions. The structure of protonated cyclopropane has been discussed thoroughly in several studies[1-4] but the evidence for the structure, formation, and even the existence of protonated cyclobutane is much less convincing.[5-10] In the present work, the protonation of cyclobutane is studied theoretically by ab initio SCF methods using a flexible basis set of atomic orbitals. The level of accuracy of the treatment is such as to provide a good assessment of the energy of protonation. In previous experimental work, Cacace et al.[9] have reported on the gas-phase protonation of cyclobutane using the helium tritide, He^3H^+, molecular ion which is an extremely strong acid. They interpret their results as direct evidence for the forma-